Birefringence determination in turbid media

Christophe Baravian* and Jérôme Dillet
Laboratoire d'Energétique et de Mécanique Théorique et Appliquée CNRS 7563, University of Nancy, France

Jean-Paul Decruppe
Laboratoire de Physique des Milieux Denses EA 3469, University of Metz, France

(Received 22 August 2006; revised manuscript received 15 December 2006; published 16 March 2007)

We study the influence of birefringence on incoherent polarized light transport in turbid media. In particular, Mueller matrices backscattered by a diffusing medium are modified by the birefringence of the suspending phase. We study this effect both theoretically, through Monte Carlo simulations, and experimentally with a highly birefringent xanthane solution in which particles are added at various concentrations to modify its turbidity. Comparisons between experiments on flow-induced birefringence of the xanthane solution with or without particles are in good agreement and show the capability of measuring birefringence in turbid media through analysis of Mueller matrices.

DOI: 10.1103/PhysRevE.75.032501 PACS number(s): 42.25.Lc, 42.25.Ja, 83.50.Ax, 78.35.+c

I. INTRODUCTION

Incoherent unpolarized light transport in opaque dispersions is well described by radiative transfer theory [1] and can be modeled by diffusion approximations which essentially depend on the mean free path of diffusive photons l_{TR} inside the medium [1–4]. The measurement principles are based on the analysis of the spatial intensity repartition of light backscattered by an opaque diffusing medium, far from a light source focused at the medium surface [4]. Also, incoherent polarized light transport can be solved using Monte Carlo simulations and has shown to be very sensitive to particle radius a and its optical refractive index [5,6]. Wang and Wang [7] showed from Monte Carlo simulations that a birefringent continuous phase can affect polarized light transport in dense turbid media through some elements of the backscattered Mueller matrix. In this article, we focus both experimentally and theoretically on these effects in very turbid media.

In the first part, the sample preparation and experimental setup for measurements of backscattered Mueller matrices are presented. In the second part, we describe Monte Carlo simulations for birefringent opaque media. Finally we show how to use Mueller matrices for birefringence determination in random media and apply it to a xanthane solution under shear.

II. METHODS

A. Sample preparation

The xanthane solution (SKW Biosystems), prepared at 10 g/l in distilled water with 0.1 mol/l of NaCl, shows a flow birefringence and a non-Newtonian shear thinning behavior. From this xanthane solution (refractive index $n=1.34$), six opaque samples are prepared by the addition of nonabsorbing particles at various mass fractions (1%, 1.25%, 1.5%, 1.75%, 2.5%, and 3%). Particles are stabilized oil droplets ($n=1.45$) from Firmenich SA with a nearly monodisperse size distribution and an average droplet radius $a=230$ nm (measured using a Malvern Mastersizer X). We checked that the presence of particles does not affect the xanthane rheology. The flow birefringence of the xanthane solution (free of particles) is measured with the technique described in [8]. As the shear rate is increased, the birefringence δ also increases, typically from 2×10^{-5} to 7×10^{-5} [Fig. 6(b)].

B. Experimental setup

The experimental setup for the measurement of Mueller matrices backscattered by turbid media is described in detail elsewhere [6]. It is based on a laser light ($\lambda'=635/1.34\approx474$ nm in the xanthane solution) focused at the medium surface. Four independent polarization states of photons entering and going out of the medium can be selected. For each couple of polarization states, the backscattered light is collected by a charge coupled device (CCD) camera. So a set of 16 images is acquired, corresponding to the various polarization states of incident and backscattered photons. Linear combinations of these images lead to the construction of the Mueller matrix (Fig. 1), which allows calculation of the electromagnetic field anywhere in the backscattered plane. In this matrix, element M_{11} corresponds to unpolarized incoherent light transport (energy). The system is embedded on a Physica MCR300 rheometer (Anton Paar), and the shear is applied by a glass plate geometry (5 cm in diameter, 2 mm gap).

C. Unpolarized incoherent light transport

The M_{11} element is well modeled by the scalar radiative transfer theory in the diffusion approximation [1,2,4]. For opaque media, the values obtained for the transport length are represented in the inset of Fig. 2, together with its calculation using Mie theory [4]. The good agreement shows that droplets remain stable when dispersed in the xanthane solution.

III. MONTE CARLO SIMULATIONS

A. Principles

Monte Carlo simulations of incoherent polarized light transport in a collection of randomly distributed spherical

*Electronic address: christophe.baravian@ensem.inpl-nancy.fr

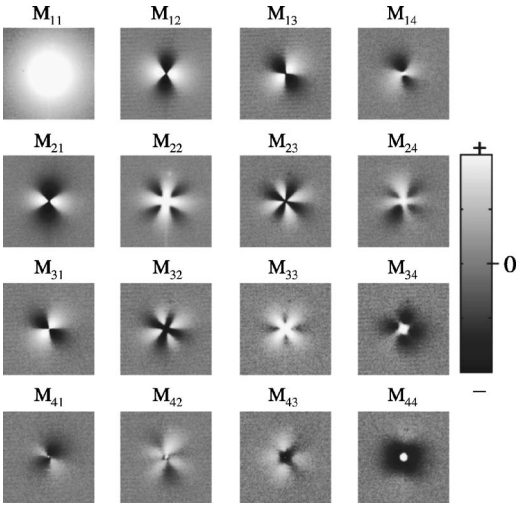

FIG. 1. Experimental backscattered Mueller matrix for 1% concentration of particles in xanthane solution at a shear rate of 606 s^{-1}. Each image size is 1 cm × 1 cm.

particles are based on successive scattering events given by Mie theory and are described in details elsewhere [5,6].

Following Wang and Wang [7], the effect of birefringence on incoherent polarized light transport is a modification of the Stokes vector along the photon traveling between two successive scattering events. This modification depends on both the photon direction (compared to the birefringence axis) and the traveling distance d_s. In Stokes formalism, the birefringence matrix $T(\beta,\Delta)$ is [7,9]

$$T(\beta,\Delta)=\begin{pmatrix}1 & 0 & 0 & 0\\ 0 & T_{22} & T_{23} & T_{24}\\ 0 & T_{32} & T_{33} & T_{34}\\ 0 & T_{42} & T_{43} & T_{44}\end{pmatrix},$$

$$T_{22}=\cos(4\beta)\sin^2(\Delta/2)+\cos^2(\Delta/2),$$

$$T_{23}=T_{32}=\sin(4\beta)\sin^2(\Delta/2),$$

$$T_{24}=-T_{42}=-\sin(2\beta)\sin(\Delta),$$

$$T_{33}=-\cos(4\beta)\sin^2(\Delta/2)+\cos^2(\Delta/2),$$

$$T_{34}=-T_{43}=\cos(2\beta)\sin(\Delta),$$

$$T_{44}=\cos(\Delta), \qquad (1)$$

where β is the azimuthal angle of the birefringence slow axis in the x-y plane and Δ is the retardation along the photon path between two scattering events:

$$\Delta=\frac{2\pi d_s}{\lambda'}\left(\frac{n_f n_s}{\sqrt{(n_s\cos\alpha)^2+(n_f\sin\alpha)^2}}-n_f\right). \qquad (2)$$

n_s and n_f are, respectively, the slow and fast refractive indices, $n_s=n_f+\delta$, and α is the angle between the birefringence slow axis and the photon direction.

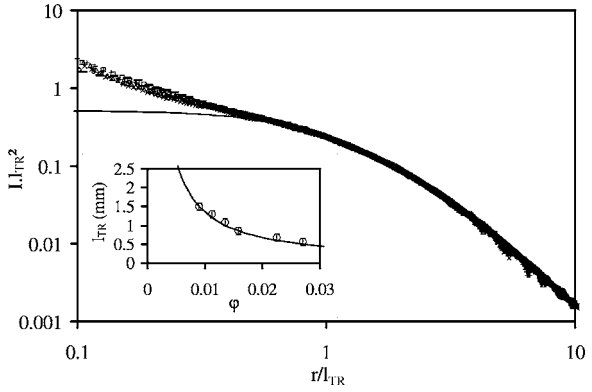

FIG. 2. Dimensionless representation of the radial intensity decrease of M_{11} elements for xanthane solution and particles at various concentrations. The solid line is the diffusion model. Inset: transport lengths from adjustment of the diffusion model on experimental data. The solid line represents Mie theory for a particle radius of 0.23 μm.

B. Analysis

From Eqs. (1) and (2), it is clear that Δ is the relevant parameter for birefringence influence on incoherent polarized light between two scattering events. To take into account the diffusive transport of retardation due to birefringence inside the medium, we consider the maximum retardation at the transport length distance: $\Delta_{TR}=2\pi\delta l_{TR}/\lambda'$.

In Fig. 3, we present results of Monte Carlo simulations in Rayleigh approximation ($a\ll\lambda'$) to show the influence of Δ_{TR} amplitude on Mueller matrices. Each image size is $10l_{TR}\times 10l_{TR}$, and the birefringence slow axis is in the horizontal x direction. Figure 3(a) corresponds to a nonbirefringent medium ($\Delta_{TR}=0$). Except for element M_{44}, the last column and last line are zero as can be deduced from symmetry constraints ([10], Chap. 17). Generally, for an isotropic medium, elements M_{14} and M_{41} are null [6,10]. When Δ_{TR} in-

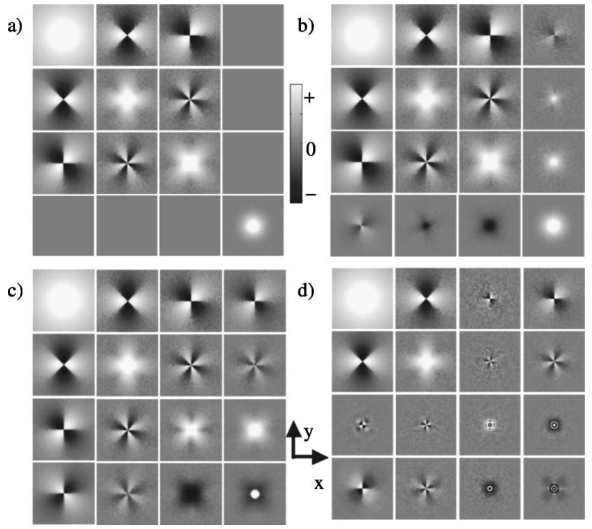

FIG. 3. Monte Carlo simulations of Mueller matrices in Rayleigh approximation. (a) $\Delta_{TR}=0$, (b) $\Delta_{TR}=0.1$, (c) $\Delta_{TR}=0.5$, and (d) $\Delta_{TR}=3$.

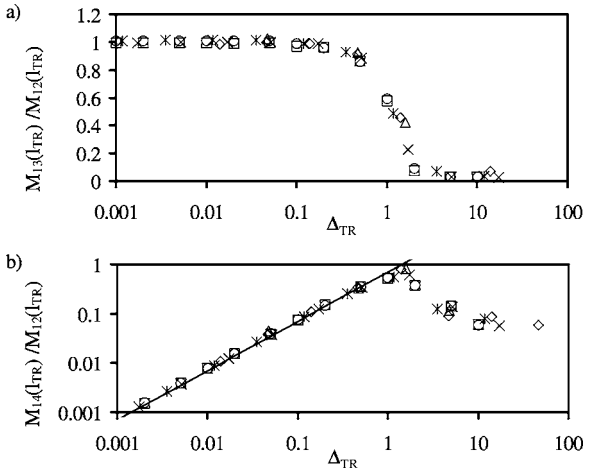

FIG. 4. Monte Carlo simulations vs $\Delta_{TR}=2\pi\delta l_{TR}/\lambda'$ for various particle sizes, birefringence values, and volume fractions [(○) 10 nm, $\varphi=1\%$; (□) 10 nm, $\varphi=5\%$; (*) 75 nm, $\varphi=1\%$; (×) 120 nm, $\varphi=1\%$; (◇) 230 nm, $\varphi=1\%$; and (△) 500 nm, $\varphi=1\%$]. (a) Amplitude of $M_{13}(l_{TR})/M_{12}(l_{TR})$ at a radial distance l_{TR}. (b) Amplitude of $M_{14}(l_{TR})/M_{12}(l_{TR})$ at a radial distance l_{TR}. The solid line corresponds to Eq. (3).

creases [Figs. 3(b) and 3(c)], the main effect of birefringence is a pattern appearance on elements M_{14} and M_{41}. For higher values above $\Delta_{TR}=1$, the effect of birefringence is to screen polarization transport [Fig. 3(d)]. Indeed, for $\Delta_{TR}>1$, polarization is randomized, since between two diffusion events (corresponding to a photon traveling a distance l_{TR}), any kind of retardation in the range $[0-2\pi]$ can be obtained. In particular, the similitude of amplitudes for elements M_{12} (or M_{21}) and M_{13} (or M_{31}) is lost. The evolution of these polarization amplitudes is studied through 60 Monte Carlo simulations, corresponding to different particle sizes (10, 75, 120, 230, and 500 nm) for various birefringence values of the suspending phase $0\leqslant\delta\leqslant0.0035$, corresponding to $0\leqslant\Delta_{TR}<100$. Also, for 10-nm particles, we perform calculations at two different volume fractions (0.01 and 0.05). Results are presented in Fig. 4. Figure 4(a) represents the amplitude at a radial distance l_{TR} of element M_{13} divided by the amplitude of element M_{12} as a function of Δ_{TR}. This ratio remains close to 1 when $\Delta_{TR}<0.5$ and drops to zero when $\Delta_{TR}\geqslant1$. Figure 4(a) therefore allows a simple experimental discrimination between the $\Delta_{TR}\leqslant1$ and $\Delta_{TR}>1$ regions.

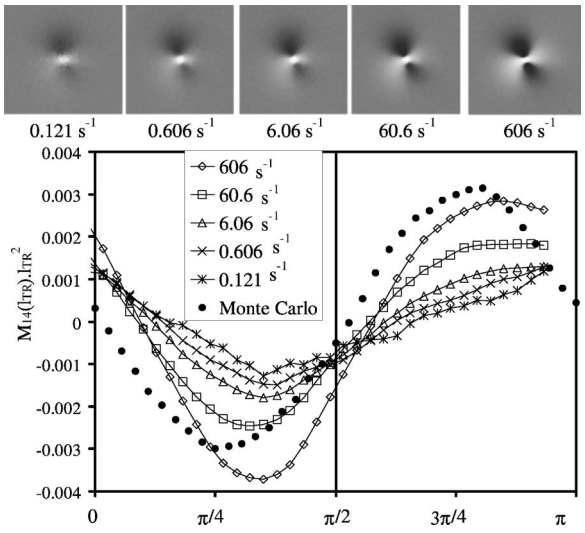

FIG. 5. Xanthane solution with a particle concentration of 1.5%. Angular variation of normalized M_{14} element at a distance $l_{TR}=1.09$ mm for various shear rates. Upper images are M_{14} elements (1 cm × 1 cm) at various shear rates. Solid symbols (●) correspond to a Monte Carlo simulation in the same conditions ($\varphi=0.015$, $a=230$ nm) with $\delta=5\times10^{-5}$.

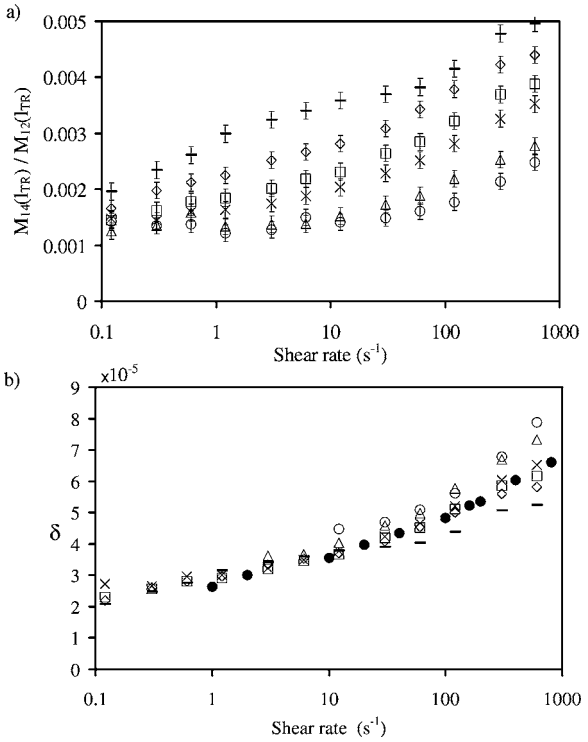

FIG. 6. Birefringence measurement in opaque media. (a) Relative amplitude of $M_{14}(l_{TR})/M_{12}(l_{TR})$ vs shear rate for different particle concentrations. (b) Birefringence measurement (−) $\varphi=1\%$, (◇) $\varphi=1.25\%$, (□) $\varphi=1.5\%$, (×) $\varphi=1.75\%$, (△) $\varphi=2.5\%$, and (○) $\varphi=3\%$). Solid symbols (●) correspond to birefringence measurements of xanthane solution without particles.

To extract the birefringence influence on polarization transport independently of the properties of the scatterers, we use the ratio of elements $M_{14}(l_{TR})/M_{12}(l_{TR})$.

Figure 4(b) shows a linear relationship between the $M_{14}(l_{TR})/M_{12}(l_{TR})$ amplitude at a radial distance l_{TR} and Δ_{TR} in the $\Delta_{TR}\leqslant1$ domain. Therefore, the determination of Δ_{TR} is straightforward in this region using the simple relation given in Eq. (3), obtained by linear regression from Fig. 4(b):

$$\Delta_{TR}=1.45M_{14}(l_{TR})/M_{12}(l_{TR}). \tag{3}$$

IV. BIREFRINGENCE MEASUREMENT IN TURBID MEDIA

The principle of birefringence measurement in opaque dispersion systems is motivated by the correlation in Fig. 4(b). From experimental Mueller matrices, the transport

length is obtained by analysis of the M_{11} element. Then the polarization amplitude in elements M_{12} and M_{13} is measured at a radial distance equal to the transport length and the ratio $M_{13}(l_{TR})/M_{12}(l_{TR})$ is checked to be close to unity (>0.9 in all our experiments). We then measure the normalized amplitude of the M_{14} element at a radial distance l_{TR}.

Figure 5 illustrates M_{14} images analysis for xanthane solution with the addition of 1.5% droplets in concentration. The amplitude of element M_{14} increases with the shear rate, corresponding to an increase of the continuous phase birefringence. The birefringence slow axis is not perfectly oriented in the velocity direction, but slightly tilted at an angle of $12° \pm 5°$ towards the vorticity direction, whereas in the Monte Carlo simulation, the slow birefringence axis is aligned in the velocity direction. So angular variation of intensity in element M_{14} gives the principal axis of the birefringence in the observation plane. For a given birefringence, increasing the volume fraction of particles decreases the transport length l_{TR} (inset in Fig. 2), and therefore $\Delta_{TR}=2\pi\delta l_{TR}/\lambda'$. At a given applied shear rate, a decrease of the amplitude of $M_{14}(l_{TR})/M_{12}(l_{TR})$ is expected while increasing the volume fraction of particles [Eq. (3)]. This effect is experimentally verified in Fig. 6(a). The birefringence of the opaque solution be can expressed, using Eq. (3), as

$$\delta = 1.45 M_{14}(l_{TR})/M_{12}(l_{TR}) \frac{\lambda'}{2\pi l_{TR}}. \quad (4)$$

Equation (4) is used to construct Fig. 6(b) from the experimental results of Fig. 6(a). The birefringence determined from Mueller matrices through Eq. (4) is in good agreement with the birefringence of the xanthane solution without particles independently measured using another technique [8].

V. CONCLUSION

We have studied the influence of the continuous phase birefringence on incoherent polarization transport. The central result is that the normalized amplitude $M_{14}(l_{TR})/M_{12}(l_{TR})$ from the Mueller matrices is proportional to the maximum retardation of light between two diffusions, $\Delta_{TR}=2\pi\delta l_{TR}/\lambda'$, and does not depend on the nature of the scatterers or their volume fraction. This technique of continuous phase birefringence determination in turbid media applies when the retardation Δ_{TR} is typically smaller than unity. It is also important to note that measurement of a Mueller matrix is completely self-sufficient for a determination of the retardation Δ_{TR} and, therefore, the birefringence amplitude and orientation.

ACKNOWLEDGMENTS

We thank Anton Paar for supporting part of this study and Dr. François Caton for useful comments and suggestions.

[1] A. Ishimaru, *Wave Propagation and Scattering in Random Media* (Oxford University Press, Oxford, 1997).
[2] R. Haskell, L. Svaasand, T. Tsay, T. Feng, and S. McAdams, J. Opt. Soc. Am. A **11**, 2727 (1994).
[3] A. Kienle and M. Patterson, J. Opt. Soc. Am. A **14**, 246 (1997).
[4] C. Baravian, F. Caton, J. Dillet, and J. Mougel, Phys. Rev. E **71**, 066603 (2005).
[5] S. Bartel and A. Hielscher, Appl. Opt. **39**, 131 (2000).
[6] J. Dillet, C. Baravian, F. Caton, and A. Parker, Appl. Opt. **45**, 4669 (2006).
[7] X. Wang and L. Wang, J. Biomed. Opt. **7**, 279 (2002).
[8] J. P. Decruppe, S. Lerouge, and H. Azzouzi1, Phys. Rev. E **71**, 011503 (2005).
[9] G. G. Fuller, *Optical Rheometry of Complex Fluids* (Oxford University Press, New York, 1995).
[10] S. Chandrasekhar, *Radiative Transfer* (Dover, New York, 1960).